

# Structure of Detonation Propagating in Lean and Rich Dimethyl Ether-Oxygen Mixtures

Rémy Mével<sup>1,2</sup>

<sup>1</sup> Center for Combustion Energy, Tsinghua University, Beijing, China

<sup>2</sup> Department of Automotive Engineering, Tsinghua University, Beijing, China

## 1 Introduction

Dimethyl ether (DME),  $\text{CH}_3\text{OCH}_3$ , demonstrates a promising potential as an alternative fuel and conventional fuel additive. The high-cetane number and low-soot tendency of DME make it attractive for cleaner diesel applications [1]. DME can be produced at the industrial scale from natural gas, coal and biomass and is foreseen as an alternative to liquefied petroleum gas (LPG) and liquid natural gas (LNG) for household combustion-based energy production in many countries such as Japan and China [2, 3]. Due to its high-potential as an alternative energy carrier, DME's combustion and kinetics properties have been extensively studied [1]. As summarized by Zhao et al., available data on DME combustion include those from flow reactor, jet-stirred reactor, shock tube, counterflow diffusion flame, and stabilized flat burner. More recently, Zhang and Ng [4] studied the explosion characteristics of DME-air mixtures, including maximum explosion pressure and pressure rise rate, flammability limits, and burning speed. The detonation properties of DME-oxygen mixtures have been investigated by Ng et al. [3]. In this latter study, Ng et al. identified non-monotonous energy release rate profiles in the ZND structure of stoichiometric and rich DME-oxygen mixtures at low-initial pressure, i.e. 5 kPa. For these mixtures, they attributed the double cell like detonation structures to the two-stage heat release whereas for lean mixtures, the multi-scale detonation feature was related to the high intrinsic instability of the detonation front [3].

The aim of the present study is to investigate the effect of the energy release profile shape on the structure of detonation propagating in DME-oxygen mixtures using one- and two-dimensional numerical simulations as well as chemical kinetics analyses.

## 2 ZND structure and energy release dynamics

The chemical structure and energy release characteristics of DME-oxygen detonation have been studied using an in-house Chemkin-based ZND code and an adiabatic constant pressure reactor approach. The reaction model used is that from Zhao et al. [1]. It is composed of 290 elementary reactions and 55 species. Note that the original thermodynamic data for  $\text{CH}_3\text{OCH}_3$  have been replaced by those from the Burcat database because of the larger temperature range over which the set of polynomial coefficients is valid.

Figure 1 presents the temperature and thermicity profiles for lean,  $\Phi = 0.5$ , and rich,  $\Phi = 2.0$ , DME-oxygen mixtures at initial pressures of 5 and 30 kPa. As observed by Ng et al. [3], the temperature profiles for the

rich mixture exhibit several inflection points which translate into two-peak energy release rate profiles, whereas for the lean mixture, monotonous energy release is seen.

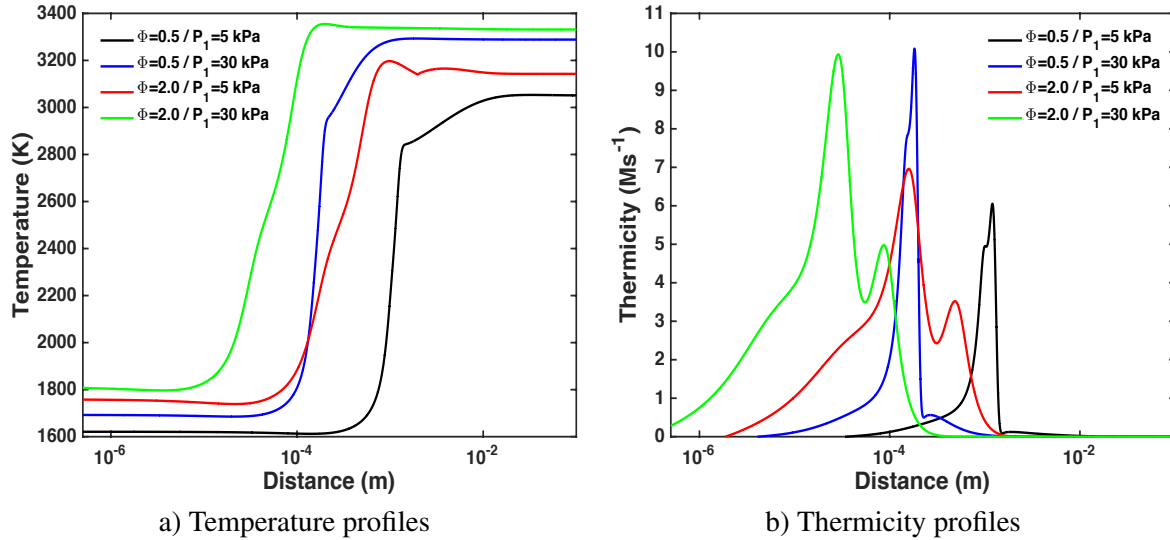


Figure 1: ZND temperature and thermicity profiles for lean and rich DME-oxygen mixtures at  $T_1=293$  K. In b), — has been multiplied by 8, — by 2, and — by 4.

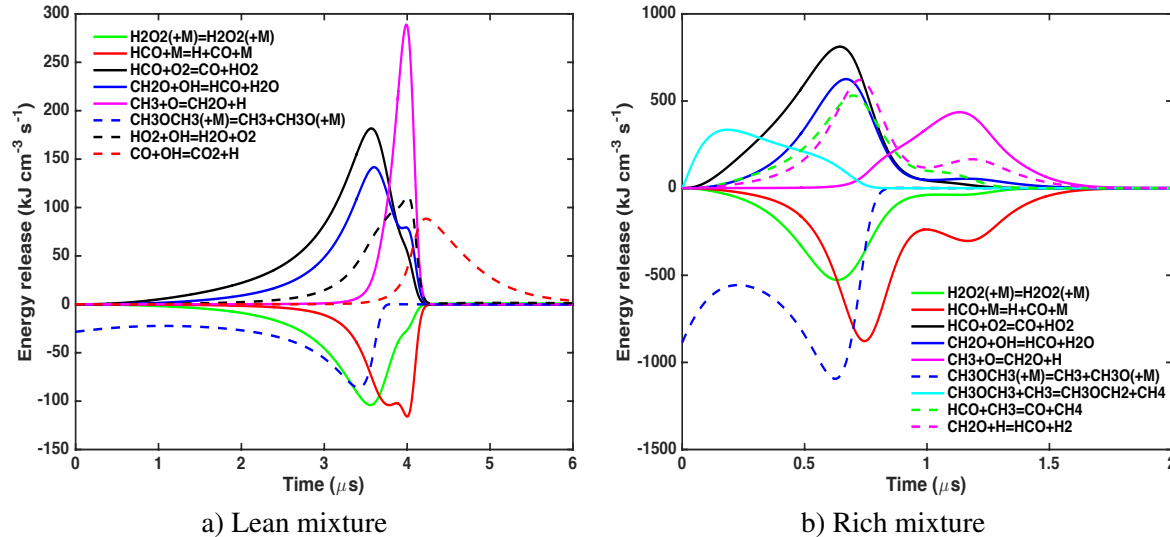


Figure 2: Energy release per reaction during the constant pressure explosion of lean and rich DME-oxygen mixtures. a)  $\Phi=0.5$ ,  $T=1621$  K,  $P=233$  kPa; b)  $\Phi=2.0$ ,  $T=1759$  K,  $P=415$  kPa.

To investigate the origin of the non-monotonous energy release in rich mixtures, we have performed an analysis of the energy release rate per reaction as shown in Figure 2. It is seen that for both lean and rich mixtures, the energy release is dominated by  $R_1$ :  $\text{HCO}+\text{O}_2=\text{CO}+\text{HO}_2$ ,  $R_2$ :  $\text{CH}_2\text{O}+\text{OH}=\text{HCO}+\text{H}_2\text{O}$  and  $R_3$ :  $\text{CH}_3+\text{O}=\text{CH}_2\text{O}+\text{H}$ . For rich mixtures, two additional reactions also contribute significantly  $R_4$ :

$\text{CH}_2\text{O} + \text{H} = \text{HCO} + \text{H}_2$  and  $\text{R}_5: \text{HCO} + \text{CH}_3 = \text{CO} + \text{CH}_4$ . For lean mixtures, the two successive steps of energy release, first step  $\text{R}_1$  and  $\text{R}_2$ , and second step  $\text{R}_3$ , are essentially coupled. The difference in time to peak is 10%, which results in a monotonous temperature profile. For the rich mixture, these two sequences appear decoupled with a difference in time to peak close to 65%.

Species profiles and reaction pathway analyses indicate that the two-step energy release feature in rich DME- $\text{O}_2$  mixtures is related to the much higher, approximately 2.5 times, concentrations of  $\text{CH}_2\text{O}$  and  $\text{CH}_4$  than in lean mixtures. Because the reactions of H atom with formaldehyde,  $\text{R}_4$ , and with methane,  $\text{R}_6: \text{CH}_4 + \text{H} = \text{CH}_3 + \text{H}_2$ , are much faster than the branching reaction  $\text{R}_7: \text{H} + \text{O}_2 = \text{OH} + \text{O}$ , the production of O atom, and thus the energy release by  $\text{R}_3$ , is delayed until both  $\text{CH}_2\text{O}$  and  $\text{CH}_4$  are consumed.

### 3 Distinguishing between single and double cellular structure

#### 3.1 Cellular structure and detonation front

To investigate the effect of the non-monotonous energy release profile in rich DME- $\text{O}_2$  mixtures, two-dimensional numerical simulations were performed using an in-house code. This code solves the 2D Euler equations with high-order (5th order WENO) schemes along with AMR (Adaptive Mesh Refinement). An implicit Runge-Kutta method (Runge-Kutta-Rosenbrock) with adaptive time step was employed to solve the stiff set of chemical ODE. Additional technical details can be found in [5]. Detonations are first propagated in 1D until an average steady-state is reached and subsequently in 2D with slight changes in the fresh mixture composition in order to trigger the detonation cellular instability. The channel is 60 mm in height. Nine AMR grid levels are used with a smallest grid size of 4  $\mu\text{m}$ . The run time is typically 2-3 weeks on 100 cores. The detailed reaction model for DME-based mixtures was reduced to 22 species and 48 reactions using the numerical procedure described by Davidenko et al. [6].

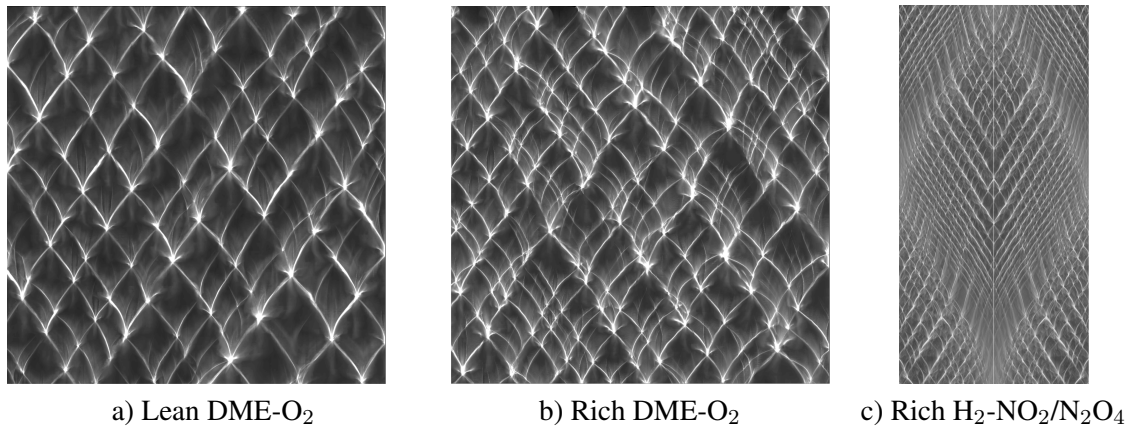


Figure 3: Numerical soot foils for detonation propagation in DME- $\text{O}_2$  and  $\text{H}_2\text{-NO}_2/\text{N}_2\text{O}_4$  mixtures. a)  $\Phi=0.5$ ,  $T_1=293$  K,  $P_1=5$  kPa; b)  $\Phi=2.0$ ,  $T_1=293$  K,  $P_1=5$  kPa; c)  $\Phi=1.5$ ,  $T_1=293$  K,  $P_1=100$  kPa. Image width: a) and b) 60 mm, c) 16 mm, taken from [7]. Propagation from bottom to top.

Figure 3 and Figure 4 show the numerical soot foils and schlieren images obtained for the lean and rich DME- $\text{O}_2$  mixtures. In addition, the numerical simulations from Davidenko et al. [7] are shown for comparison since a double cellular structure was unambiguously demonstrated both experimentally [8, 9] and

numerically [7] for such rich  $\text{H}_2\text{-NO}_2/\text{N}_2\text{O}_4$  mixtures. Both soot foils and schlieren images appear quite different for the two fuels considered in the numerical simulations. The numerical soot foils in  $\text{DME-O}_2$  exhibit a distribution of cell size with a single dominant length scale. Within some of the cells, sub-structures can be observed especially in the rich mixture. The sub-structures appear less abundant than for very lean  $\text{H}_2\text{-N}_2\text{O}$  [7] which can be explained by the much higher instability level of these mixtures, Ng's stability parameter  $\chi \sim 25$ , as compared to  $\text{DME-O}_2$  mixtures,  $\chi \sim 4\text{-}12$  [3]. The numerical soot foils for  $\text{DME-O}_2$  based mixtures appear overall more regular with fewer sub-structures than observed experimentally [3]. The soot foil obtained for  $\text{H}_2\text{-NO}_2/\text{N}_2\text{O}_4$  mixtures clearly exhibits two dominant length scales of very different size which is characteristic of a double cellular structure. These two dominant length scale are also clearly observed in the schlieren images, Figure 4 c), where Mach reflection structures of small size are present at the detonation front which is itself constituted of a Mach reflection of much larger size. The detonation front in  $\text{DME-O}_2$  mixtures appears as a rather irregular succession of incident shocks and Mach stems and do not demonstrates distinct length scales.

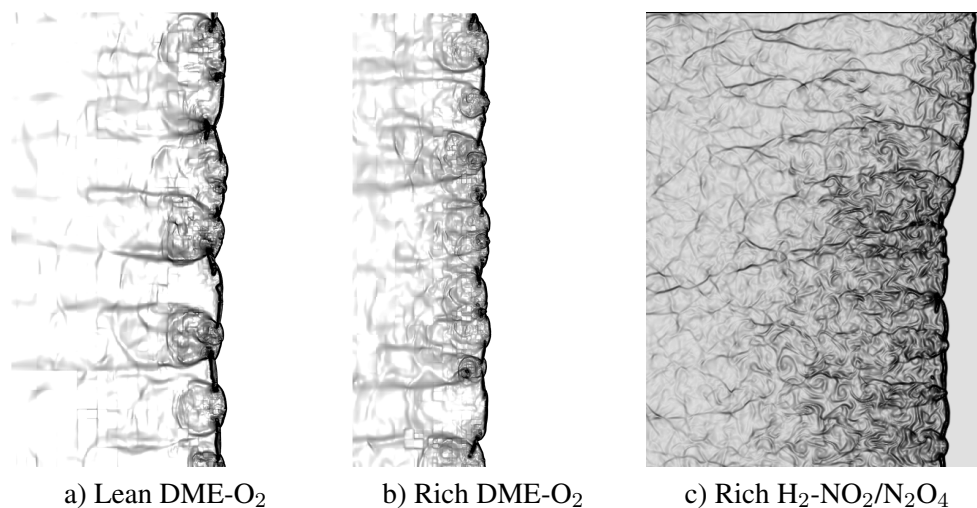


Figure 4: Numerical schlieren images for detonation propagating in  $\text{DME-O}_2$  and  $\text{H}_2\text{-NO}_2/\text{N}_2\text{O}_4$  mixtures. a)  $\Phi=0.5$ ,  $T_1=295$  K,  $P_1=5$  kPa; b)  $\Phi=2.0$ ,  $T_1=293$  K,  $P_1=5$  kPa; c)  $\Phi=1.5$ ,  $T_1=293$  K,  $P_1=100$  kPa. Image height: a) and b) 60 mm, c) 8 mm, taken from [7]. Propagation from left to right.

### 3.2 Analysis of the chemical scales

Guilly et al. [10] investigated the conditions for the existence of a double cellular structure using 2-D numerical simulations. By calibrating independently the reaction rates of their 2-step reaction model, they demonstrated the critical importance of the induction zone length and energy release rate ratios on the nature, single or double, of the detonation cellular structure. Consequently, it is interesting to compare these ratios for a number of chemical systems which exhibit non-monotonous energy release. In addition to rich  $\text{DME-O}_2$ , a number of mixtures have been considered for this analysis including very lean  $\text{H}_2\text{-N}_2\text{O}$ ,  $\text{H}_2\text{-NO}_2/\text{N}_2\text{O}_4(-\text{Ar})$ ,  $\text{CH}_4\text{-NO}_2/\text{N}_2\text{O}_4$ ,  $\text{C}_2\text{H}_6\text{-NO}_2/\text{N}_2\text{O}_4$  and  $\text{CH}_3\text{NO}_2\text{-O}_2(-\text{Ar})$ . With the exception of very lean  $\text{H}_2\text{-N}_2\text{O}$  mixtures [7, 11], the double cellular structure has been clearly established for all these chemical systems [8, 9, 12–15]. To perform these simulations, an updated version of Mével et al.'s model [16, 17],

which includes 131 species and 993 reactions, has been used. The original model was updated based on the studies of Mathieu et al. [18, 19] on  $\text{H}_2\text{-O}_2\text{-NO}_2$  and  $\text{CH}_3\text{NO}_2\text{-O}_2$  mixtures.

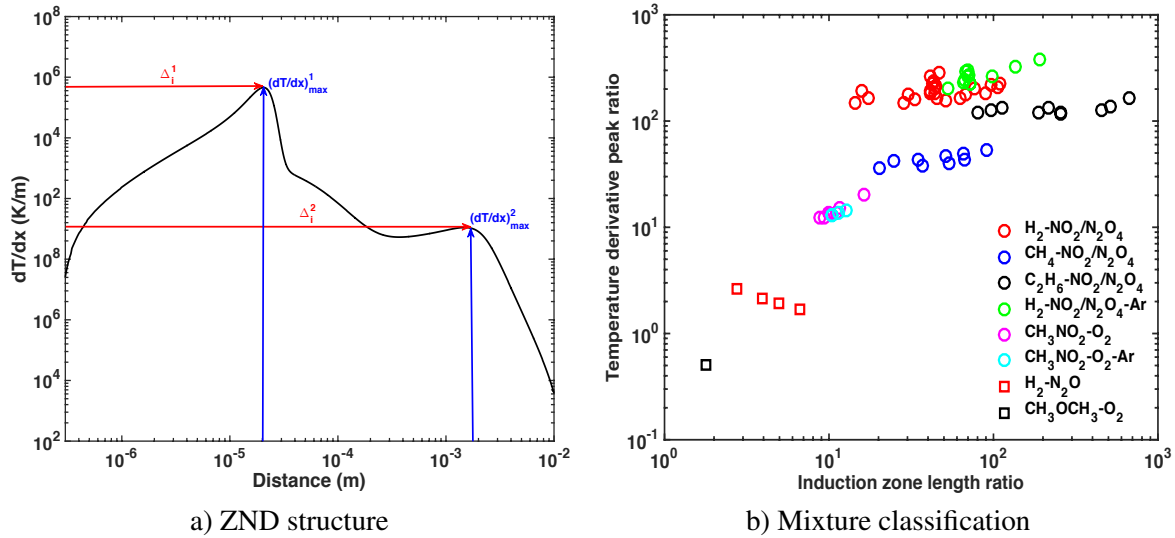


Figure 5: a) Definition of the induction length and temperature increase rate scales. b) Location of different mixtures exhibiting non-monotonous energy release in the (Induction zone length ratio, Temperature derivative ratio) plan based on ZND structure analysis. Conditions in a):  $\text{H}_2\text{-NO}_2/\text{N}_2\text{O}_4$ ,  $\Phi=1.5$ ,  $T_1=293$  K,  $P_1=100$  kPa. Conditions in b):  $\text{DME-O}_2$ :  $\Phi=2$ ,  $T_1=293$  K,  $P_1=5$  kPa;  $\text{H}_2\text{-N}_2\text{O}$ :  $\Phi=0.06\text{-}0.1$ ,  $T_1=295$  K,  $P_1=71$  kPa;  $\text{CH}_3\text{NO}_2\text{-O}_2$ :  $\Phi=1.3\text{-}1.75$ ,  $T_1=343\text{-}383$  K,  $P_1=$  kPa,  $X_{Ar}=0\text{-}0.5$ ;  $\text{H}_2\text{-NO}_2/\text{N}_2\text{O}_4$ :  $\Phi=0.8\text{-}1.7$ ,  $T_1=293$  K,  $P_1=15\text{-}200$  kPa,  $X_{Ar}=0\text{-}0.5$ ;  $\text{CH}_4\text{-NO}_2/\text{N}_2\text{O}_4$ :  $\Phi=1.05\text{-}1.6$ ,  $T_1=293$  K,  $P_1=50\text{-}100$  kPa;  $\text{C}_2\text{H}_6\text{-NO}_2/\text{N}_2\text{O}_4$ :  $\Phi=1\text{-}1.7$ ,  $T_1=293$  K,  $P_1=50\text{-}100$  kPa.

As illustrated in Figure 5 a), the ZND profiles with non-monotonous energy release were characterized using two ratios: (i) the ratio of temperature increase rates,  $R(TI)=((dT/dx)_{max}^1/(dT/dx)_{max}^2)$ , and the ratio of induction lengths  $R(\Delta_i)=\Delta_i^2/\Delta_i^1$ , where the superscripts 1 and 2 refer to the first and second energy release step, respectively. The position of the different mixtures in the  $(R(\Delta_i), R(TI))$  plan is shown in Figure 5 b). For all mixtures with double cellular structure, both  $R(\Delta_i)$  and  $R(TI)$  are above 10 whereas for the rich  $\text{DME-O}_2$  mixture,  $R(\Delta_i)=1.77$  and  $R(TI)=0.51$ . This seems to indicate that the two steps of energy release in the rich  $\text{DME-O}_2$  mixture are not separated enough nor different in amplitude enough to enable the formation of a detonation with double cellular structure which is consistent with the numerical soot foil and schlieren images.

## 4 Conclusion

The structure of detonations propagating in  $\text{DME-O}_2$  mixtures of different equivalence ratios has been investigated through ZND and 2-D numerical simulations. Whereas lean mixtures exhibit monotonous temperature profiles, rich mixtures demonstrate two-step energy release. Both 2-D numerical soot foils and schlieren fields obtained for  $\text{DME-O}_2$  were compared to those obtained for  $\text{H}_2\text{-NO}_2/\text{N}_2\text{O}_4$  mixtures, for which a double cellular structure has been clearly established. This comparison seems to indicate that  $\text{DME-O}_2$  mixtures exhibit classical detonation structure with sub-structures rather than a double cellular

structure. Analysis of the ZND profiles indicates that detonations in DME-O<sub>2</sub> do not present the same characteristics as detonations in fuel-NO<sub>2</sub>/N<sub>2</sub>O<sub>4</sub> and CH<sub>3</sub>NO<sub>2</sub>-O<sub>2</sub> mixtures in terms of induction zone lengths and temperature derivatives ratios. The numerical soot foils and schlieren images show that sub-structures are more abundant in rich than in lean DME-O<sub>2</sub> mixtures. The impact of non-monotonous energy release on the formation of sub-structures needs to be clarified.

## References

- [1] Zhao Z. et al. (2008). *International Journal of Chemical Kinetics*, 40:1.
- [2] Chen Z. et al. (2007). *Proceedings of the Combustion Institute*, 31:1215.
- [3] Ng H.D. et al. (2008). *Fuel*, 88:124.
- [4] Zhang B. and Ng H.D. (2016). *Energy*, 107:1.
- [5] Gallier et al. (2017) *Proceedings of the Combustion Institute*, 35:In press.
- [6] Davidenko D. et al. (2009). *Proceedings of the European Combustion Meeting*, 4.
- [7] Davidenko, D. et al. (2011). *Shock Waves*, 21:85.
- [8] Joubert F. (2001). PhD Thesis: Université de Poitiers. 150 p.
- [9] Joubert F. et al. (2008). *Combustion and Flame*, 152:482.
- [10] Guilly V. et al. (2006). *Comptes Rendus de Mécanique*, 334:679.
- [11] Pfahl U. et al. (1998). Technical Report: FM-98-5, EDL, Caltech.
- [12] Luche J. et al. (2006). *Comptes Rendus de Mécanique*, 334:323.
- [13] Virot F. et al. (2010). *Shock Waves*, 20:457.
- [14] Sturtzer M.-O. et al. (2005). *Shock Waves*, 14: 45.
- [15] Karnesky J. and Shepherd J. (2008). 32nd Int. Symp. Comb.: Work in Progress Poster.
- [16] Mével R. et al. (2009). *Proceedings of the Combustion Institute*, 32:359.
- [17] Mével R. and Shepherd J.E. (2015). *Shock Waves*, 25:217.
- [18] Mathieu O. et al. (2014). *Proceedings of the Combustion Institute*, 34:633.
- [19] Mathieu O. et al. (2016). *Fuel*, 182:597.